Peer-reviewed version available at Sensors 2018, 18, 3981; doi:10.3390/s18113981

Article

A Novel Device-Free Counting Method based on Channel Status Information

Junhuai Li [1,2], Pengjia Tu [1], Huaijun Wang [1,2,*], Kan Wang [1,2] and Lei Yu [1,2]

[1] School of Computer Science and Engineering, Xi'an University of Technology; Xi'an 710048, China
[2] Shaanxi Key Laboratory for Network Computing and Security Technology; Xi'an 710048, China
* Correspondence: lijunhuai@xaut.edu.cn ; Tel.: +029-823-12012

Abstract: Crowd counting is of significant importance for numerous applications, e.g., urban security, intelligent surveillance and crowd management. Existing crowd counting methods typically require specialized hardware deployment and strict operating conditions, thereby hindering their widespread deployment. To acquire a more effective crowd counting approach, a device-free counting method based on Channel Status Information (CSI) is proposed, which could mitigate environment noise through wavelet transform and extract the amplitude or phase covariance matrix as the feature vector. Moreover, both the spatial diversity and frequency diversity are leveraged to improve detection robustness. The accuracy of the proposed CSI-based method is compared with a renowned crowd counting one, i.e., Electronic Frog Eye: Counting Crowd Using WiFi (FCC). The experimental results reveal an accuracy improvement of 30% over FCC.

Keywords: wavelet transform; covariance matrix; spatial diversity; frequency diversity; robustness

1. Introduction

In some overpopulated countries, the contradiction between the limited indoor space and large population is becoming increasingly prominent. Thus, it is of vital significance to implement crowd counting in public places, e.g., libraries, museums, shopping malls and college classrooms, which are with limited resources and strong mobility. Meantime, it is a crucial and challenging task to acquire the human traffic or accurately calculate the population in some particular circumstances. Therefore, signal changes caused by human motion has been utilized to acquire crowd counting [1]. Since crowd counting can lead to an efficient utilization of space resources, it has been widely applied to intelligent surveillance, guided to tour, crowd management and urban security, etc.

Numerous crowd counting approaches have emerged over the past decades, e.g., video-based recognition, infrared-based induction, and non-image-based localization. However, these methods all require specialized hardware deployment and strict operating conditions which hinder their wide deployment. First, video-based recognition has the advantages of high-accuracy, rapidness and low-cost, and is applicable to various commercial and security fields. However, it is encountered by some constrains, e.g., many blind spots cannot be monitored and the environmental requirements are high [2]. Second, although infrared-based induction has also been widely applied in markets, subways and buses, it will be challenging to obtain a high counting accuracy, when the people flow becomes denser [3]. Third, non-image-based solutions typically require people to carry wearable devices. Unfortunately, it is impractical and expensive to distribute equipments to each individual in a public place, and is not feasible under an emergent event [4,5].

The legacy crowd counting methods not only consume the manpower and materials, but also encounter the statistical error. In recent years, Wireless Sensor Network (WSN) technology has been gradually applied from theoretical research to industries. Besides, some network technologies, e.g., Wi-Fi., are also utilized in the field of crowd counting. The Received Signal Strength Indicator (RSSI) could realize crowd counting from the perspective of localization [6] and estimate human position in small areas or homes [7]. However, the RSSI is only applicable to the MAC layer information at

Peer-reviewed version available at Sensors 2018, 18, 3981; doi:10.3390/s18113981

the packet level, and its value will not remain stable with time fluctuation, and meanwhile does not provide sufficient recognition and robustness in complex indoor environments, thus the counting error will exist. Nowadays, some commercial ordinary wireless network cards (such as 802.11 a/g/n networks) can provide both amplitude and phase information on different subcarriers, utilizing the form of Channel State Information (CSI) by Orthogonal Frequency Division Multiplexing (OFDM). Different from RSSI, the CSI is a type of physical layer information and could obtain matrix of all subcarriers from transmit antennas to receive antennas [8]. More importantly, the CSI acquired by different subcarriers would exhibit distinct fading. These fading can be suppressd by the Multiple Input Multiple Output (MIMO) technique(such as IEEE 802.11n, 3GPP LTE, and mobile WiMAX systems), which can increase the capacity, range and reliability of wireless systems from the space dimension [9]. MIMO could enhance data throughput and transmission distance, without additional bandwidth and transmission power. Thus, CSI has both frequency diversity provided by OFDM and spatial diversity supplied by MIMO. As the specific RSSI at the physical layer, CSI is expected to enable more accurate and reliable detections, which has also attracted intensive attentions from both academic and industrial domains, and thus it would be a promising one in crowd counting.

The main contributions of our work are listed as follows:

- We present a novel device-free counting method on the basis of CSI. Both the space diversity provided by MIMO and frequency diversity supplied by OFDM subcarriers are explored to obtain more accurate and robust recognition.
- Different from the transparent amplitude or phase information, we eliminate random noise with the wavelet transforms, and then extract either the amplitude or phase covariance matrix as the feature vector to enable counting.
- On one hand, we compare the differences and similarities between phase and amplitude information in crowd detection; on the other hand, as compared to the FCC system, we collect 0-10 different volunteers walking data, the experiment results reveal that the proposed method could be significantly improved in terms of accuracy, scalability and reliability, and could be enhanced by space diversity and frequency diversity meanwhile .

2. Related works

Compared to RSSI, CSI is the estimation of channel information on each subcarrier, and it could also characterize the frequency selective fading characteristics of Wi-Fi channels. In addition, CSI involves the amplitude and phase information on each subcarrier, providing rich frequency domain information. Next, existing works on different approaches of CSI will be summarized.

The amplitude-based detection. Amplitude-based scheme attracts more attentions in recent years since it is sensitive to adjacent humans, while unrelated background noise remains relatively stable. In this context, Xiao et al. [10] proposed a CSI feature extraction model based on the first and second largest eigenvalues of the Pearson correlation matrix of CSI amplitude, to detect the presence of human. The existence detection is performed by outlier identification using normal features of density-based clustering. In [11], a monotonic function was proposed to depict the relationship between the crowd number and CSI amplitude variation. The function can be leveraged by a new dilated CSI matrix of the percentage of nonzero elements and the Grey Verhulst Model. In [12], a system was proposed to capture the variance between CSI amplitude of each subcarrier as features and uses Hidden Markov Model (HMM) to detect the human movement with different speed followed by a speed independent device free entity detection. In E-eyes [13], the distribution of CSI amplitude was utilized to classify the activities in entire home environment and identifies activities by calculating the similarity of each CSI segment and pre-structured activity files. Han et al. [14] designed a device-independent passive fall detection system using time stability and frequency diversity of CSI amplitude, in view of the fact the static human body is independent of the time domain variation of wireless signals. Experimental results in [14] showed that Wi-Fall can achieve a detection accuracy of 87%.

The Amplitude and Phase-based detection. Despite the fact that quite a few works have studied CSI for device-free detection, most previous studies only utilize the amplitude information but not the phase information. However, in [15], it was found that the CSI phase information is more sensitive to the detection process. Therefore, both the amplitude and phase information are utilized to calculate the maximum eigenvalues of Pearson correlation matrices, in order to compose a two-dimensional feature to infer the existence of a moving human body. This paper further employed an SVM machine learning model to achieve human moving detection. In [16], a new feature with the coefficient of phase variation was defined. The coefficient of phase variation is the ratio of the standard deviation to the mean of the CSI phase, in which human movement is detected when the averaged ratio is set within a predefined confidence interval. Qian et al. [17] proposed a device-free PAssive detection of moving humans with Dynamic Speed (PADS). The features are extracted from the covariance matrices of both CSI amplitude and phase, then calculated the eigenvalues of both matrices, and selected the maximum and second maximum eigenvalue of each matrix to form a four-tuple of features, and meanwhile chosen the SVM classifier to detect humans.

In existing works, the CSI phase information has attracted significant attentions. In order to further illustrate its availability, we attempt to respectively utilize the amplitude and phase information of CSI to achieve the counting, and meanwhile exploit the frequency diversity and spatial diversity of CSI to obtain more accurate and robust detection, which has significant improvement in accuracy, scalability and reliability in crowd counting.

3. Crowd Counting based on CSI

3.1. Architecture

Figure 1 shows the system architecture of this paper, and the system architecture consists of two stages: (1) data preprocessing and (2) learning algorithm. To verify the validity of the architecture, we perform a series of experiments to examine the relationship between CSI changes and the number of moving people.

First, we obtain CSI observations with different numbers and then filter out both phase and amplitude noise from original CSI observations through the wavelet transform. For phase information, it first needs to be a linear transformation.

Second, following the data preprocessing, we further extract the covariance matrix as the feature value from both the amplitude and phase information, respectively.

Finally, the covariance matrix will be used as the initial values of the crowd counting method, and meanwhile multiple antennas are introduced to enhance the detection accuracy and robustness.

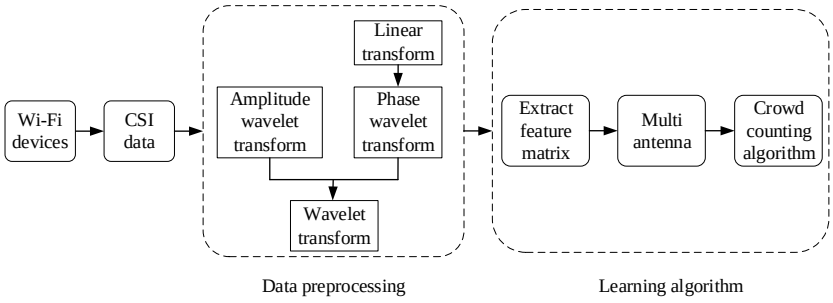

Figure 1. System architecture

3.2. Data Preprocessing

Although standard wireless network cards provide RSSI information, the RSSI is only a rough estimate of the wireless channel, and it does not involve the specific number of antennas and subcarriers.

Peer-reviewed version available at Sensors 2018, 18, 3981; doi:10.3390/s18113981

Nowadays, some common IEEE 802.11n standard commercial wireless network cards began to emerge, which could provide detailed amplitude and phase information on different subcarriers in the form of CSI. The CSI is a type of physical layer information on the subcarrier scale, referring to the channel characteristics of a communication link. This type of information describes how the signal passes through the air from transmitter to receiver, and reflects the fading factor of signal on each transmission path, environmental degradation, signal scattering, power attenuation with distance, etc.

In the narrow-band flat fading channel, the OFDM system in the frequency domain is modeled as

$$y = Hx + N, \tag{1}$$

where y, x, H and N are respectively denoted as the receive vector, the transmit vector, the channel matrix and the additive white Gaussian noise (AWGN) vector.

Next, the CSI message, which represents the channel response of multiple subcarriers, is divided into 30 groups. Hence, the CSI value with $N = 30$ groups collected at the receive that can be represented as

$$\begin{aligned} H(f_i) &= \|H(f_i)\| e^{jsin(\angle H(f_i))}, \\ i &\in [1, 30], \end{aligned} \tag{2}$$

where $H(f_i)$ is the CSI at the subcarrier with the carrier frequency f_i, $\angle H(f_i)$ denotes its amplitude value and $\|H(f_i)\|$ denotes its phase value.

Environmental factors (such as temperature, lighting and room settings) might appear with outliers in the CSI measurements, and these outliers would affect the detection performance to some extent. Thus, the measurements of amplitude and phase of CSI will be the basic input for our method, which would be through a wavelet transform process beforehand. The wavelet transform removes the observation value with larger deviations and meanwhile restore original signals as much as possible.

Given the original signal C_φ , $\varphi(t)$ constitutes the fundamental wavelet, i.e., if $\varphi(t)$ meets (3)

$$C_\varphi = 2\pi \int_{-\infty}^{+\infty} \frac{\varphi(w)^2}{|w|} dw < \infty, \tag{3}$$

then the continuous wavelet transform $f(t)$ can be written as

$$\begin{aligned} W_f(a,b) &= \frac{1}{\sqrt{C_\varphi}} - \frac{1}{\sqrt{|a|}} \int_{-\infty}^{+\infty} f(t) \overline{\varphi}(\frac{t-b}{a}) dt, \\ a, b &\in R, a \neq 0, \end{aligned} \tag{4}$$

where $\bar{\varphi}$ denotes the conjugate of φ , and R represents a real number set.

The associated inverse transformation formula $f(t)$ can be written as

$$f(t) = \frac{1}{\sqrt{C_\varphi}} \int_{-\infty}^{+\infty} db \int_{-\infty}^{+\infty} W_f(a,b) |a|^{-\frac{1}{2}} \varphi(\frac{t-b}{a}) \frac{da}{a^2}. \tag{5}$$

In the following, Figure 2 illustrates the original CSI amplitude and phase as well as their wavelet transformed graph, respectively. From Figure 2, it is observed that the graph curve become smoother after the signal is filtered by the wavelet, and the frequent random fluctuations are filtered out. Thus, the wavelet transform can effectively filter out interference signals. It can be also revealed that the denoised signal retains the basic characteristics of the original one as well.

3.3. Feature Extraction

A suitable feature plays a key role. Nowadays, various statistical feratures [18–20] have been exploited for detection, such as the *variance*, *mean*, *std*, $Max - Min$. Unfortunately, it is possible that

Preprints (www.preprints.org) | NOT PEER-REVIEWED | Posted: 1 August 2018 doi:10.20944/preprints201808.0015.v1

Peer-reviewed version available at Sensors 2018, 18, 3981; doi:10.3390/s18113981

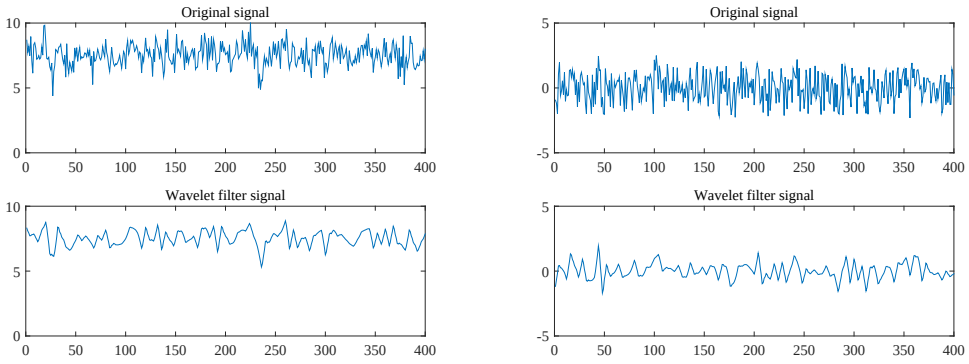

(a) (b)

Figure 2. Comparison between the original and wavelet filter signal. (**a**) amplitude; (**b**) phase

these statistical features could not directly for crowd counting. Henceforth, we propose to extract the amplitude and phase covariance matrix as the feature vector to achieve counting. Then, the corresponding feature vector can be represented as

$$\begin{aligned} a(i,j) &= cov(\angle H(i), \angle H(j)), \\ b(i,j) &= cov(\|H(f_i)\|, \|H(f_j)\|), \end{aligned} \tag{6}$$

where $\angle H(i)$, $\|H(f_i)\|$ are the phase and amplitude information, respectively.

In the following, A and B are utilized to denote the amplitude and phase covariance matrix, respectively, i.e.,

$$\begin{aligned} A &= [a(i,j)]_{N*N}, \\ B &= [b(i,j)]_{N*N}, \end{aligned} \tag{7}$$

where $a(i,j)$ and $b(i,j)$ denote the phase and information covariance between vectors i and j, respectively.

Both Figure 3, 4 show the variation of CSI amplitude values with different numbers of moving people. Herein, Figure 3 demonstrates the CSI changes with one antenna when 0, 2 people are walking, respectively, and Figure 4 displays the change with three antennas. The X-axis denotes the package index, while the Y-axis denotes the CSI amplitude value. For both cases, it can be clearly observed that the different degree of change of the CSI amplitude with the number of people increases. Therefore, the amplitude information can be considered as means of the crowd counting.

Since there exist the random noise and unsynchronized time clock, the raw phase information is unavailable, as shown in Figure 5a. However, most existing works also involve the phase information [15,16] [21,22]. One of the most important reasons is that the phase information is more sensitive. In our work, in order to achieve people counting through the phase information, we employ a linear transformation to remove random noise from the raw phase values. The measured phase $\hat{\boldsymbol{\phi}}_i$ for the i^{th} subcarrier can be expressed as

$$\hat{\boldsymbol{\phi}}_i = \boldsymbol{\phi}_i + 2\pi k_i \triangle t + 2\pi k_i \triangle w, \tag{8}$$

where $\boldsymbol{\phi}_i$ is the raw phase. $2\pi k_i \triangle t$ and $2\pi k_i \triangle w$ are the unknown phase shifts caused by the clock offset t and frequency difference w, respectively.

To remove the impact of random noise, the linear transformation can be written as

$$\bar{\boldsymbol{\phi}} = \hat{\boldsymbol{\phi}}_i - \alpha k_i - \beta, \tag{9}$$

Preprints (www.preprints.org) | NOT PEER-REVIEWED | Posted: 1 August 2018 doi:10.20944/preprints201808.0015.v1

Peer-reviewed version available at Sensors 2018, 18, 3981; doi:10.3390/s18113981

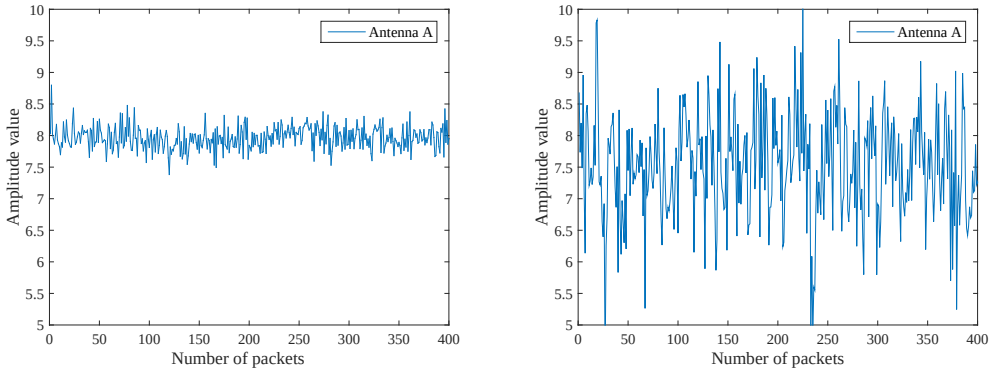

Figure 3. CSI changes with number of people at one antenna. (**a**) zero people; (**b**) two people

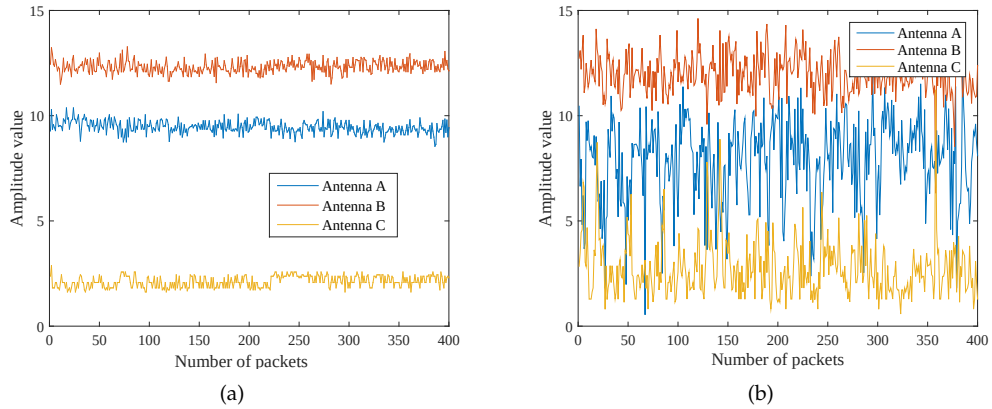

Figure 4. CSI changes with number people at three antenna. (**a**) zero people; (**b**) two people

where α and β denote intuitively the slope and offset of phase change over all subcarriers, respectively, $\bar{\boldsymbol{\phi}}$ is the random phase offset which have been removed. Figure 5b illustrates an example of the phase after transformation, which is stably distributed.

3.4. Crowd Counting Algorithm

Our work aims to achieve crowd counting in specific scenarios, and the CSI information of the PHY layer information is more susceptible to environmental changes. PEM, presented in [11], can adaptively reflect the relationship between CSI changes and the number of people in a short time. As such, it is intuitive to represent different numbers of people. Nevertheless, the FCC system [11] only considers amplitude information and directly uses the raw amplitude, i.e., the CSI phase information is ignored. Therefore, we propose to further improve the FCC system. In particular, it is proposed to mitigate the environmental noise by the wavelet transform, extract CSI amplitude and phase covariance matrix as feature matrices and convert them into two-dimensional matrix, and expand the matrices and calculate the elements percentage. In the proposed algorithm, $C[i][j]$ represents the processed two-dimensional matrix $(S \times P)$, with and being the number of subcarriers and packets, respectively. C_{min} and C_{max} are the maximum and minimum value of covariance matrix, respectively, and D is the dilatation coefficient.

The aforementioned crowd counting approach can be listed as follows:

Preprints (www.preprints.org) | NOT PEER-REVIEWED | Posted: 1 August 2018 doi:10.20944/preprints201808.0015.v1

Peer-reviewed version available at Sensors 2018, 18, 3981; doi:10.3390/s18113981

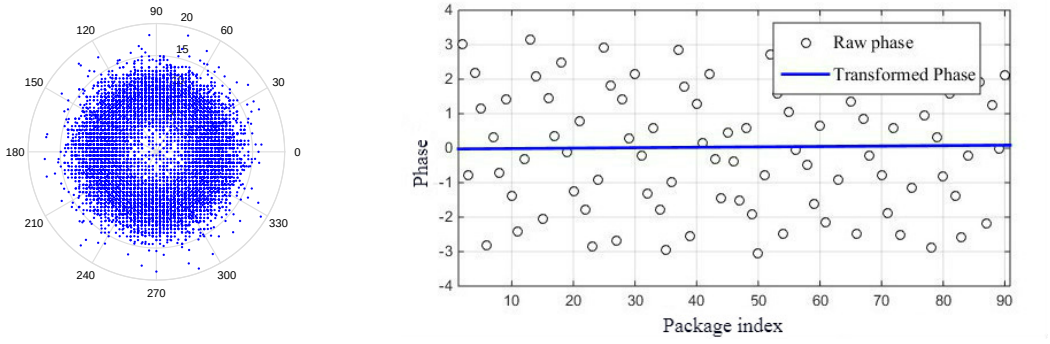

(a) (b)

Figure 5. Raw phase information and the calibrated version. (**a**) the groups of random raw phase values; (**b**) linear transformation phase

- We adopt the wavelet transforms to remove the random noise, and then extract both the CSI amplitude and phase covariance matrix as the feature vector.
- All elements in the CSI amplitude or phase covariance matrix M_0 are initialized to "0", and each CSI value $C[i][j]$ is converted into integer k by $k = \lfloor \frac{C[i][j]-C_{min}}{C_max-C_{min}} \cdot (R-1) \rfloor + 1$. Then, the elements in row k and column j of elements is set to be "1".
- The elements within the coverage of D is set to "1", called matrix expansion. The size of the expansion is related to the dilatation coefficient D , and all element within the coverage with a radius of D are set to "1". After dilation, the covariance matrix M_0 is transformed into a dilated covariance matrix M . The matrix M is occupied by more "1", and usually comes along with the CSI changes drastically.
- The number of "1" in the expand covariance matrix M is counted, and the percentage of non-zero elements in the matrix M of each subcarrier is calculated. This percentage can reveal the change of CSI, and it can also represent the number of moving people.

3.5. Leveraging Space Diversity

Since multiple antennas are adopted in more and more popular MIMO communication systems, the signal strength variability can be reduced based on small scale fading compensation. It is worth mentioning that multiple antennas can provide spatial diversity for CSI. In MIMO system, both the transmitter and receiver have multiple antennas, and the combination of each receive and transmit antenna can be considered as a stream. Due to different propagation paths of diverse streams in the indoor environment, the CSI received by different antennas are differentiated. Therefore, $H(f_i)$ is with pxq dimensions and can be represented as

$$H(f_i) = \begin{bmatrix} h_{11} & h_{12} & \cdots & h_{1q} \\ h_{21} & h_{22} & \cdots & h_{2q} \\ \vdots & \cdots & \cdots & \vdots \\ h_{p1} & h_{p2} & \cdots & h_{pq} \end{bmatrix}, \tag{10}$$

where h_{pq} is complex numbers representing the amplitude and phase of each subcarrier for an antenna, and p,q indicate the number of transimit and receive antennas, respectively.

As such, multiple antennas are exploited to increase the reliability via spatial diversity and improve via spatial multiplexing without enhancing the bandwidth and transmission power [23,24]. Figure 6a shows the characteristic distribution with different numbers of the amplitude covariance matrix, while the phase covariance matrix is displayed in Figure 6b. It can be observed that the phase

Preprints (www.preprints.org) | NOT PEER-REVIEWED | Posted: 1 August 2018 doi:10.20944/preprints201808.0015.v1

Peer-reviewed version available at Sensors 2018, 18, 3981; doi:10.3390/s18113981

Algorithm 1 Crowd Counting based on Channel State Information

Require: Sample Data ([H_1,H_2,⋯,H_k], $k \in (1,30)$), Matrix Resolution (R), Dilatation Coefficient (D), Number of Subcerriers (S), Number o packets (P), Covariance Matrix ($C(i,1)$), Maximum Value of covariance (Cmax), Minimum Value of covariance (Cmin), Expansion Matrix (M)

Ensure: Percentage of Element (q)

```
The covariance matrix is extracted from wavelet transformed data
for i = 1 to S do
    The integer K is calculated
    The matirx M is dilated        // the element in row k and column j is set to be "1"
     for u = -D to D do
         for v = -D to D do
             The matirx M is dilated  // the element in a radius of D is set to be "1"
         end for
     end for
end for
for l = 1 to P do
    for h = 1 to S do
        M = M (1, h)               // the percentage of the matrix M of each subcarrier
        q = q / (P*S)              // the percentage is calculated
    end for
end for
```

value of all antennas remains relatively stable across different scenarios, but the amplitude values of all three antennas pose significant differences. The result shows that the selected features of amplitude and phase vary as the number of antennas changes. Therefore, the antenna is utilized mistakenly, and then significant false might occur.

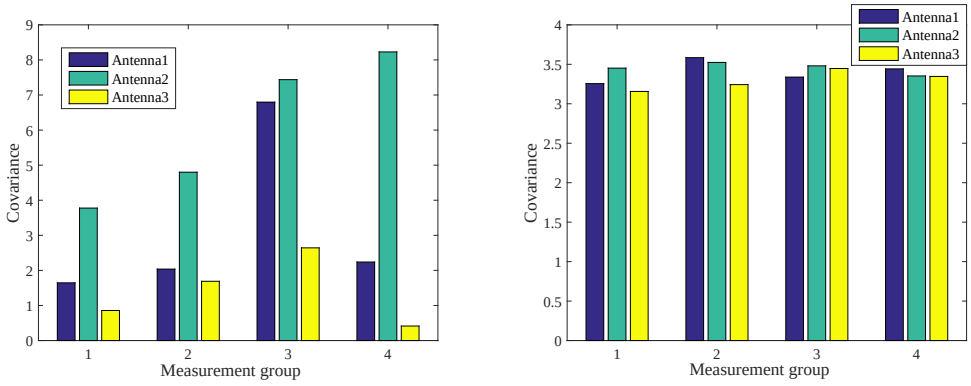

Figure 6. Antenna diversity. (**a**) antenna diversity of amplitude feature; (**b**) antenna diversity of phase feature

4. Experiment Results and Analysis

4.1. Experiment setup

To evaluate the performance of proposed approach, a real experiment on commercial 5300 wireless net cards is conducted, and we utilize two-antenna AP-link wireless router as transmitter and the PC with three antennas as receiver, as illustrated in Figure 7a. The data from 0-10 different volunteers is

Peer-reviewed version available at Sensors 2018, 18, 3981; doi:10.3390/s18113981

collected in the 6th Teach Building of Xi'an University of Technology. Figure 7b shows a sample of different volunteers. The transmitter continuously sends packets to the receiver, whenever different volunteers walk through the monitoring area. Finally, the 4min data is collected at each sample point and 400 stable data samples are selected in the intermediate state.

In different situations, both AP and PC are placed at the height of 1.5m, and their separate distance is 3.5m. Different volunteers randomly move about 3m in the proximity of communication link and 4min data is collected as the sample data at the same experimental environment.

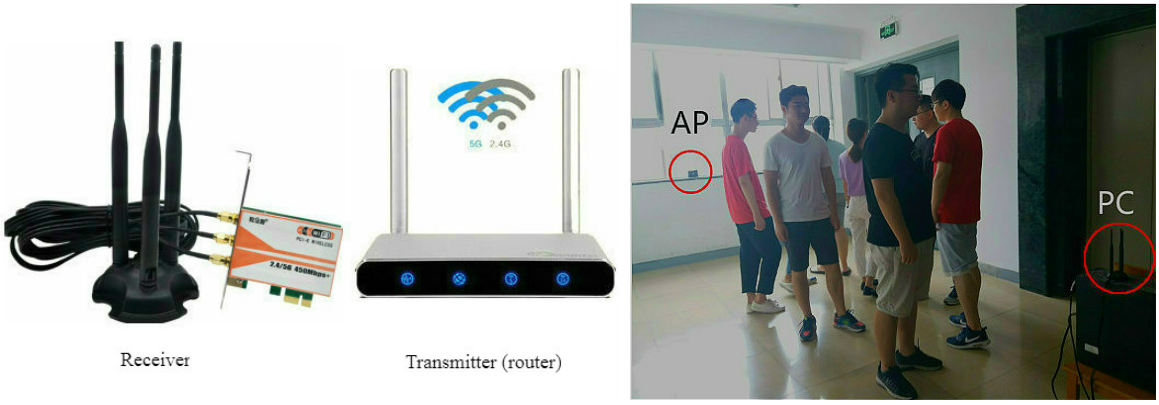

Figure 7. Equipment and scene. (**a**) receive and router; (**b**) experimental scene

4.2. Impact of Dilatation Coefficient

The dilation coefficient plays an important part in our work. Figure 8 shows the impact of dilatation coefficient. It can be seen that the expansion percentage increases with the growth of dilatation coefficient, when the matrix resolution R is constant. Although there is great difference for the percentage when the number of people is different, it would not induce detection errors. Figure 8a, b show the variation on the percentage of amplitude and phase (under different dilatation coefficient D), respectively.

When $D = 0$, the percentage remains constant with the increase in the number of people, since each column has only one non-zero element before dilatation. When $D = 20$, the percentage also keeps constant. It is because that the dilatation coefficient D would result in a tendency of 100% for the percentage. Thus, if D is excessively either high or low, then it will affect the detection results. However, when D is equal to 5, 10 and 15, although there exists a monotone increase between percentage and number of people, the curve track is different. Therefore, the different dilation coefficients will bring different experimental results. In our work, $D = 10$ is set as the dilation coefficient.

4.3. Relation between population and amplitude (or phase)

Figure 9 shows three different monotonous relations between the percentage and three different antennas configurations. Among them, Figure 9a reveals that the CSI amplitude change can be detected when 0, 1, 2 and 3 people are walking, and Figure 9b shows the CSI phase changes. Although there is a monotonic relationship between amplitude and phase, the curve track of amplitude and phase changes are different, and the different antennas configurations also present the diverse trajectories.

4.4. Comparison of Different Features

In this work, both the CSI phase and amplitude covariance matrices are extracted to achieve crowd counting. Figure 10a compares the differences of the mean of the amplitude and phase covariance

Preprints (www.preprints.org) | NOT PEER-REVIEWED | Posted: 1 August 2018 doi:10.20944/preprints201808.0015.v1

Peer-reviewed version available at Sensors 2018, 18, 3981; doi:10.3390/s18113981

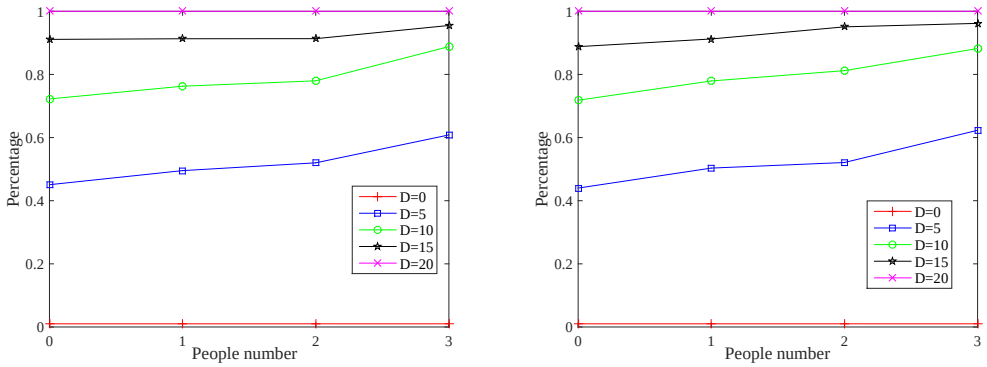

Figure 8. The impact on dilatation coefficient. (**a**) amplitude; (**b**) phase

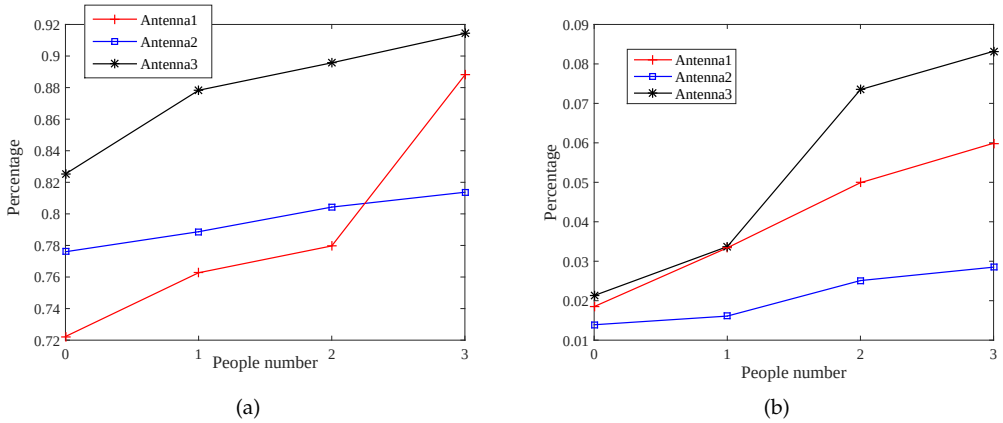

Figure 9. Monotonic. (**a**) amplitude; (**b**) phase

matrix. It can be observed that the amplitude information is with a large fluctuation, while the phase information fluctuate is relatively stable. Figure 10b shows the percentage difference of crowd counting between amplitude and phase. It can be observed that the growth gets slower from the sixth person for the amplitude information, while the phase starts to grow slowly from the ninth person. Thus, the phase information can detect more people, and is more reliable and sensitive. Both Figure 10c, d show the performance difference between the proposed method with the FCC system. Regardless of either amplitude or phase information, the proposed method can detect more people than the that in FCC system with a higher detection accuracy. For the FCC system, the phase arrives at a certain threshold from the fourth person, while our method reaches a certain threshold from the seventh person. The similar case occurs for the amplitude likewise. In other words, although the percentage increases as the number of moving people grows, it would be saturated when the crowd density reach a certain threshold.

5. Conclusions

Crowd counting plays a key role in many applications, but existing counting methods usually require specialized hardware deployment and strict using conditions which hinder their wide deployment. Therefore, a Device-Free Counting Method based on Channel Status Information is proposed. From the similarities and differences of amplitude and phase changes that CSI phase has higher detection accuracy and sensitivity. Comparing the proposed method with FCC systems in the

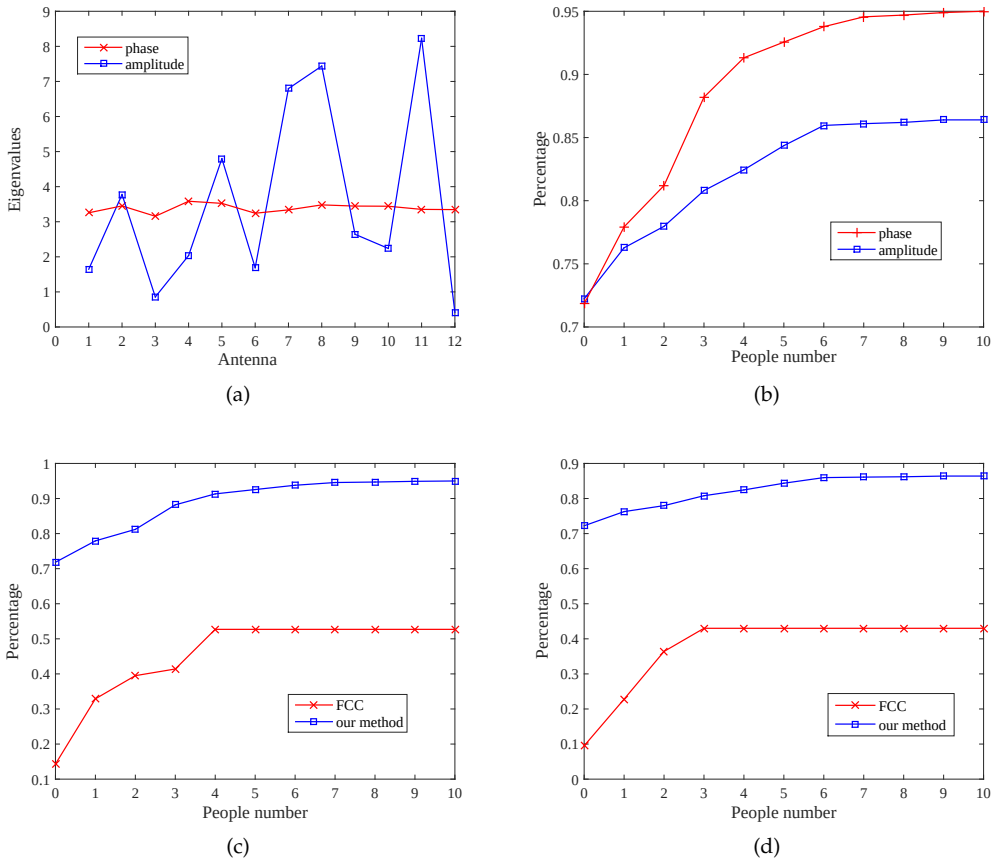

Figure 10. Comparison of different features. (**a**) eigenvalue of covariance matrix on different antennas; (**b**) different percentages of amplitude and phase; (**c**) FCC and our method about amplitude; (**d**) FCC and our method about phase

same experimental environment, it can be observed that the proposed method can detect more people and have higher counting accuracy, regardless of either the amplitude or phase covariance matrix as the feature vector. In the next step, a method should be proposed to accurately estimate the population in the special environment with more people. Moreover, the more accurate method will be studied when the target has different speeds.

Author Contributions: Li Junhuai and Tu Pengjia conceived the idea, conducted the investigation. Tu Pengjia collected data, conducted the experiments and wrote the paper. Wang Huaijun provided supervision and guidance during the work and did the project management. Wang Kan helped Tu Pengjia to improve the quality of the work. Yu Lei validated the idea to the work.

Funding: This work was supported by the National Key Research and Development Plan (No.2017YFB1402103), Natural Science Foundation of China (No.61172018, 61771387), Scientific Research Program of Shaanxi Province(2016KTZDNY01-06, 2018HJCG-05), Project of Xi'an science and technology planning foundation (XALG035), CERNET Innovation Project (No.NGII20160704), and Xi'an BeiLin Science Research Plan (No.GX1626, GX1623). The authors are grateful for the anonymous reviewers who made constructive comments.

Acknowledgments: The authors are grateful for the anonymous reviewers who have made constructive comments.

Conflicts of Interest: The authors declare no conflict of interest

References

1. Zou, H.; Zhou, Y.; Yang, J.; Gu, W.; Xie, L.; Spanos, C. FreeCount: Device-Free Crowd Counting with Commodity WiFi[C]. *In Processings of the IEEE Global Communications Conference*. **2017**, 1-6.

2. Zhao, X.; Delleandrea, E.; Chen, L. A People Counting System Based on Face Detection and Tracking in a Video[J]. *Computer Engineering*. **2017**, 38, 67-72.
3. Wu, H.; Gao, C.; Cui, Y.; W, Ru. Multipoint infrared laser-based detection and tracking for people counting[J]. *Neural Computing & Applications*. **2018**, 29, 1405-1416.
4. Kannan, P.; Padmanabha, S.; Venkatagiri, S.; Chan, M.; Ananda, A.; Peh, L. Low cost crowd counting using audio tones[C]. *In Proceedings of the 10th ACM Conference on Embedded Network Sensor Systems, ACM: New York, NY, USA,* **2012**, pp.155-168.
5. Li, F.; Zhao, C.; Ding, G.; Gong, J.; Liu, C.; Zhao, F. A reliable and accurate indoor localization method using phone inertial sensors[C]. *In Proceedings of the 2012 ACM Conference on Ubiquitous Computing, ACM: New York, NY, USA,* **2012**, pp.421-430.
6. Rani, T.; Jayakumar, C. Unique identity and localization based replica node detection in hierarchical wireless sensor networks[J]. *Computers & Electrical Engineering*. **2017**, 64, 148-162.
7. Oguchi, K.; Shou, M.; Dai, H. Human positioning estimation method using received signal strength indicator (RSSI) in a wireless sensor network[J]. *Procedia Computer Science*. **2014**, 34, 126-132.
8. Gong, L.; Yang, W.; Zhou, Z.; Man, D.; Cai, H.; Zhou, X.; Yang, Z. An adaptive wireless passive human detection via fine-grained physical layer information[J]. *Ad Hoc Networks*. **2016**, 38, 38-50.
9. Xiao, J.; Wu, K.; Yi, Y.; Wang, L.; M.Ni, L. FIFS: Fine-grained indoor fingerprinting system[C]. *In Proceedings of IEEE ICCCN*. **2012**, 1-7.
10. Xiao, J.; Wu, K.; Yi, Y.; Wang, L.; M.Ni, L. FIMD: Fine-grained Device-free Motion Detection[C]. *In Proceedings of IEEE ICPDS* . **2013**, 229-235.
11. Xi, W.; Zhao, J.; Li, X.; Zhao, K; Tang, S; Liu, X; Jiang, Z. Electronic frog eye: Counting crowd using WiFi[C]. *In Proceedings of IEEE INFOCOM*. **2014**, 361-369.
12. Lv, J.; Yang, W.; Gong, L.; Man, D.; Du, X. Robust WLAN-Based Indoor Fine-Grained Intrusion Detection[C]. *In Proceedings of IEEE GLOBECOM,*. **2016**, 1-6.
13. Wang, Y.; Liu, J.; Chen, Y.; Gruteser, M.; Yang, J.; Liu, H. E-eyes: device-free location-oriented activity identification using fine-grained WiFi signatures[C]. *In Proceedings of the 20th annual international conference on Mobile computing and networking, ACM: New York, NY, USA,* **2014**, pp.617-628.
14. Wang, Y.; Wu, K.; Lionel, M. WiFall: Device-free fall detection by wireless networks[C]. *In Proceedings of IEEE INFOCOM*. **2014**, 271-279.
15. Wu, C.; Yang, Z.; Zhou, Z.; Liu, X.; Liu, Y.; Cao, J. Non-Invasive Detection of Moving and Stationary Human With WiFi[J].*IEEE Journal on Selected Areas in Communications*. **2015**, 33, 2329-2342.
16. Gong, L.; Yang, Wu.; Man, D.; Dong, G.; Yu, M.; Lv, J. WiFi-Based Real-Time Calibration-Free Passive Human Motion Detection†[J]. *Sensors*. **2015**, 15, 32213-32229.
17. Qian, K.; Wu, C.; Yang, Z.; Liu, Y.; Zhou, Z. PADS: Passive detection of moving targets with dynamic speed using PHY layer information[C]. *In Proceedings of IEEE ICPADS*. **2014**, 1-8.
18. Sobron, I.; Ser, J.; Eizmendi, I.; Velez, M. Device-Free People Counting in IoT Environments: New Insights, Results and Open Challenges[J]. *IEEE Internet of Things Journal*. **2018**, 1-1.
19. Chen, Y.; Shen, C. Performance Analysis of Smartphone-Sensor Behavior for Human Activity Recognition[J]. *IEEE Access*. **2017**, 5, 3095-3110.
20. Gupta, P.; Dallas, T. Feature Selection and Activity Recognition System Using a Single Triaxial Accelerometer[J]. *IEEE Transactions on Biomedical Engineering*. **2014**, 61, 1780-1786.
21. Chapre, Y.; Ignjatovic, A.; Seneviratne, A.; Sanjay, Jha. CSI-MIMO: Indoor Wi-Fi fingerprinting system[C]. *In Pcoceedings of IEEE Local Computer Networks*. **2014**, 202-209.
22. Wu, C.; Yang, Z.; Zhou, Z.; Qian, K.; Liu, Y.; Liu, M. PhaseU: Real-time LOS identification with WiFi[C].*In Proceedings of IEEE INFOCOM*. **2015**, 2038-2046.
23. Xu, C.; Firner, B.; Robert, S.; Moore.; Zhang, Y.; Trappe, W.; Howard, R.; Zhang, F.; An, N. SCPL: Indoor device-free multi-subject counting and localization using radio signal strength[C]. *In Proceedings of ACM/IEEE IPSN*. **2013**, 79-90.
24. Zhu, H.; Xiao, F.; Sun, L.; Wang, R.; Yang, P. SCPL: R-TTWD: Robust Device-Free Through-The-Wall Detection of Moving Human With WiFi[J]. *IEEE Journal on Selected Areas in Communications*. **2017**, 1090-1103.